TX Beamforming EVM Performance of a 65 dBm-EIRP Slant-Polarized Gapwaveguide Phased Array at 28 GHz

Citation for the original published paper (version of record):
Bagheri, A., Karlsson, H., Bencivenni, C. et al (2023). TX Beamforming EVM Performance of a 65 dBm-EIRP Slant-Polarized Gapwaveguide Phased Array at 28 GHz. 17th European Conference on Antennas and Propagation, EuCAP 2023.
http://dx.doi.org/10.23919/EuCAP57121.2023.10133798

(article starts on next page)

TX Beamforming EVM Performance of a 65 dBm-EIRP Slant-Polarized Gapwaveguide Phased Array at 28 GHz

Alireza Bagheri*,†, Hanna Karlsson*, Carlo Bencivenni*, Jose-Ramon Perez-Cisneros‡, Parastoo Taghikhani‡, Christian Fager‡, and Andrés Alayón Glazunov†
*Gapwaves AB, Göteborg, Sweden, {alireza.bagheri, hanna.karlsson, carlo.bencivenni} @gapwaves.com
†University of Twente, Enschede, Netherlands, a.alayonglazunov@utwente.nl
‡Chalmers University of Technology, Göteborg, Sweden, {jospere, parastoo, christian.fager} @chalmers.se

***Abstract*—The transmit error vector magnitude (EVM) performance measurements of a slant-polarized 28 GHz gapwaveguide-based phased array is analyzed in this paper. The performance is studied by using a large range of signals, with varied powers, symbol rates, and quadrature amplitude modulation (QAM) orders. The measurements have been conducted for four different scanning angles. A non-standardized over-the-air (OTA) link between the phased array and the receiver in a laboratory environment is used. The results show that the phased array antenna supports a 31 dB effective isotropic radiated power (EIRP) dynamic range at a maximum 2% EVM when transmitting a 64-QAM modulated signal with 250 MS/s symbol rate at all scanning directions.**

***Index Terms*—EVM, EIRP, phased array, 5G, mmWave.**

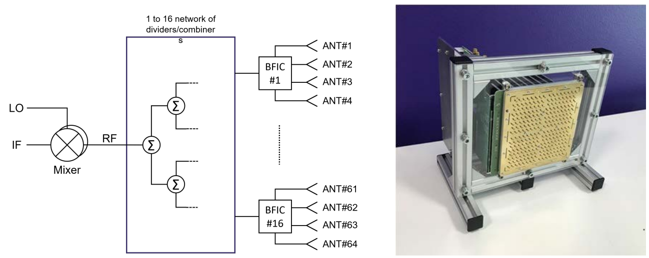

(a) (b)

Fig. 1. (a) Schematic of the beamforming network of the phased array, (b) fabricated prototype of the 16×16, 65 dBm-EIRP slant-polarized gapwaveguide phased array with operating frequency from 26.5 – 29.5 GHz and 2D beam scanning capability [4].

I. Introduction

Wireless communications technology is rapidly occupying the millimeter wave (mmWave) frequency bands because of the available electromagnetic spectrum for 5G and 6G outdoor and indoor communications. The 5G standard allocates the bands from 23.5–30.5 GHz, 37–43 GHz, and 57–71 GHz; the first two bands are for licensed operation, while the latter is unlicensed. High data rates are aimed to be delivered by large phased array antennas that can serve several spatially dispersed users at the same time. Currently developed 5G phased arrays are capable to deliver high equivalent isotropic radiated power (EIRP) of the order of 60 dBm or higher, required to overcome the large propagation path loss at the mmWaves [1]. Several examples of phased array designs for the aforementioned frequencies demonstrating high performance can be found in [2], [3] and the references therein.

Here we consider the design presented in [4], which is based on the gapwaveguide transmission line technology [5]. The gapwaveguide technology uses an engineered Artificial Magnetic Conductor (AMC) surface that prevents field leakage without the need for a metallic contact [6]. Some of the benefits that this technology offers are low losses equivalent to conventional waveguides, high isolation and cavity modes suppression, and a simplified assembly of multi-layer structures as well as enabling mass production by means of moulding or die-casting. Other phased array antennas based on the gapwaveguide technology can be found in [7], [10].

The high data rate performance of a phased array is primarily determined by the linearity and signal-to-noise (SNR) performance of the chipsets used in the design of the phased array antenna system, the performance of which is beyond our scope. On the other hand, the Error Vector Magnitude (EVM) is a measure of the difference between the ideal transmit symbols and the measured symbols after the equalization. Modulation quality is defined by the difference between the measured carrier signal and a reference signal. Hence, data transmission quality can be expressed in terms of the EVM [8]. The EIRP of a beam produced by a phased array depends on the realized array gain times the input power delivered by the power amplifiers to an antenna element (can be a sub-array, i.e., smaller array) divided by the feeding losses.

In this paper, we present (non-standardized) over-the-air (OTA) measurements over a short indoor link showing radiation patterns, EIRP, and EVM versus scan angle. We show that the design of a low profile, low structure complexity, phased array antenna system with high EIRP, up to 60.5 dBm, and low EVM, i.e., less than 2 % is feasible at the mmWave frequencies for the considered scenario [4].

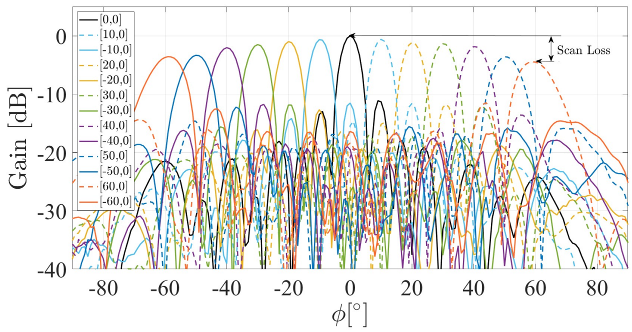

(a)

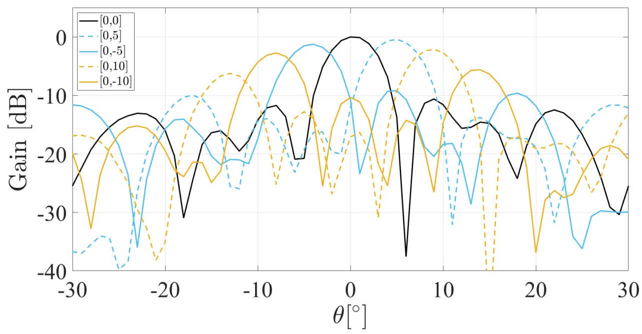

(b)

Fig. 2. Measured normalized beamforming gain patterns of the phased (a) as a function of the azimuth angle and elevation angle corresponding to broadside direction (The definition of scan loss is shown in the plot.), (b) as a function of the elevation angle and azimuth corresponding to the broadside direction.

II. Phased Array Antenna System

The evaluated phased array antenna is low-profile with 16×16 45°-polarized elements which comprise only two layers. The PCB consists of only 6 layers, which is much lower compared to other wideband 28 GHz phased arrays available in the literature (see the works cited above). The antenna system supports a full scanning range in azimuth, i.e., 120°, while the scanning in elevation covers a 20° field of view. The maximum EIRP is 65 dBm. A sketch of the array antenna beamforming network is shown in Fig. 1(a). The array employs four mmWave frequency highly-integrated silicon up/down converter ICs (UDC) (not shown in the sketch). Each UDC has a 1×4 local oscillator (LO) multiplier [9], they serve a quarter of the array, and the structures of all quarters are comparable. The phased array comprises 16 beamformer integrated circuits (BFICs) that are connected to 4 antenna elements each, i.e., in a 1×4 architecture. Fig. 1(b) shows a picture of a prototype. A further description of the design of the phased array antenna system as well as the experimental performance verification can be found in [4].

Fig.2(a) and (b) show the normalized radiation patterns of the array an in both the azimuth and in the elevation, respectively. The patterns were measured at 28 GHz. The scanning in azimuth is shown for the elevation angle in the broadside direction of the array, which is also taken as a reference for scanning in elevation. As can be seen in Fig. 2 the scanning performance is good with little antenna gain scan loss. The present paper focuses only on the scanning performance over the azimuth because a similar analysis can be repeated at the elevation too. The scan loss is 0.4, 1.8 and 4 dB at azimuth scan angles 20°, 40°, and 60°, respectively. The steering angle accuracy is also good, which is much better in azimuth than in elevation. A full evaluation of the scanning accuracy of the array is presented in [4]. In the next sections, we evaluate the EVM in an indoor (non-standardized) OTA measurement setup for broadside radiation and scanning angles in azimuth.

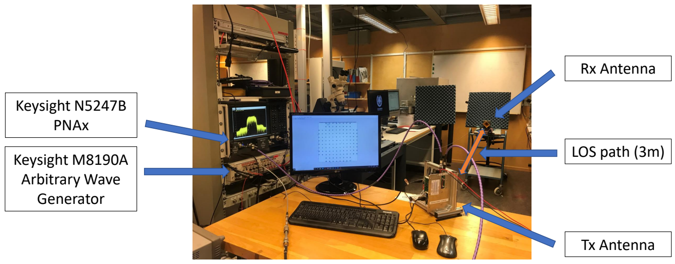

Fig. 3. Schematic representation of the non-standardized over-the-air (OTA) measurement setup in an indoor environment.

III. Measurement Setup

The capability of the proposed phased array to sustain a high data rate link was verified by performing over-the-air (OTA) measurements in the transmit (TX) mode. The complex modulation performance of the phased array was evaluated using the measurement setup shown in Fig.3. An Agilent Arbitrary Waveform Generator (AWG) model M8190A is used to generate a complex modulated signal at the intermediate frequency (IF) of 2.62 GHz. The AWG generates QAM-modulated waveforms with different symbol rates, and with a pulse-shaping filter (root raise cosine filter) of $\alpha = 0.35$. A Keysight PNA-X Network Analyzer model N5247B was connected to the receive (RX) standard horn antenna. The transmit (TX) radio frequency (RF) signal was a single frequency within the operation band of the phased array from $26.5-29.5$ GHz. The RX signal is demodulated and compared with the TX signal, which is done with a MATLAB program. The horn antenna has a gain of 25 dBi and is placed at a 3 m distance in the line of sight path with respect to the phased array's main beam. The PNA-X also functions as a local oscillator at 6.595 GHz and is connected to the phased array's LO port.

IV. Results and Analysis

Various combinations of the system parameters were used to study the EVM and EIRP interrelationship. Four azimuth scanning angles were considered, i.e., 0° (broadside direction, no scanning), 20°, 40°, and 60°. Four quadrature amplitude modulation (QAM) constellation orders were considered, namely, $16-$QAM, $64-$QAM, $128-$QAM, and $256-$QAM.

TABLE I
EIRP VALUES OF THE PHASED ARRAY AT 28 GHz.

AWG (mVpp)	200	400	600	800
AWG (dBm)	-10	-4	-0,5	2
Pin (dBm)	-17	-11	-7,5	-5
EIRP* (dBm) @ 0°	49	55	58,5	60,5
EIRP (dBm) @ 20°	48,6	54,6	58,1	60,1
EIRP (dBm) @ 40°	47,2	53,2	56,7	58,7
EIRP (dBm) @ 60°	45	51	54,5	56,5

*The relation between input power and EIRP @ 0° is provided in [4].

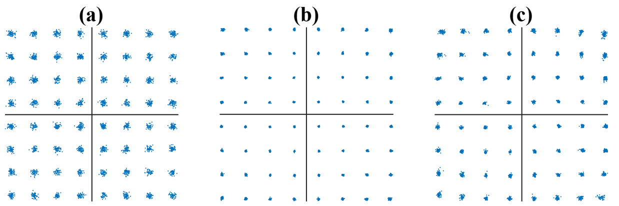

Fig. 4. Measured constellation errors for a 64−QAM modulated transmission at 500 MS/s (equivalent to 3 Gbps transmission rate) (a) EVM=3.1 % and EIRP=18 dBm, (b) EVM=1.2 % and EIRP=55 dBm, and (c) EVM=2.6 % and EIRP=60.5 dBm (at 5 dB back-off from saturation). See Fig. 3 for OTA measurement.

In order to study the impact of the noise three different IF (AWG) bandwidths of the modulated signals were used: 100, 250, and 500 MS/s. The input signal voltage of AWG was varied at four levels: 200, 400, 600, and 800 mVpp (mVpp = millivolts peak to peak). The signal is fed to the phased array through a coaxial cable with 7 dB insertion loss at 28 GHz. The EIRP associated with AWG levels are provided in Table I. All combinations of the above cases have been measured.

First, we consider the case when the phased array is radiating at the broadside angle (i.e., no scanning with azimuth and elevation angles both equal to 0° in Fig. 2). The EIRP values are 19, 55, and 60.5 dBm (the first one has been achieved with 30 dB attenuating the AWG's 200 mVpp signal and the latter one corresponds to a 5 dB back-off from saturated EIRP as shown in [4]). The corresponding measured error vector magnitude (EVM) values are 3.1, 1.2, and 2.6 %, respectively. The data rate of the signal is 3 Gb/s computed for a transmission of a 64−QAM modulated signals at a symbol rate of 500 MS/s and the signal bandwidth is 675 MHz.

Fig. 4 shows the constellations of the 64−QAM modulated signals with the EIRP and EVM values mentioned above. As can be seen from Fig. 4 signal distortion in the link as measured by the EVM is very low. The relatively higher EVM value, i.e. more distortion, at low EIRP is due to the dominance of noise in the system. Meanwhile, at high EIRP non-linearity of amplifiers in the phased array distorts the signal.

Next, we consider the measured EVM while scanning the beam. Fig. 5 shows the EVM as a function of EIRP based on measurements employing a 64−QAM modulated signal with 250 MS/s and centered at 28 GHz. The measurements were performed at broadside, i.e., 0° in azimuth and elevation and an azimuth scanning angle at 60°. The latter is the largest steering angle of the devised phased array antenna. It should be noted that additional measurements were performed employing attenuators in order to obtain lower EIRP values than the ones generated by means of the AWG.

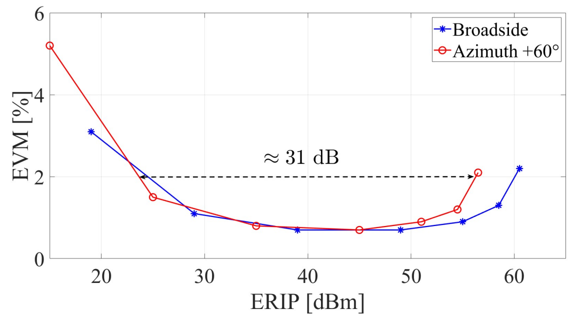

Fig. 5. TX EVM vs. EIRP measured over-the-air at a 3 m TX-RX separation for a 64−QAM modulated transmission at 250 MS/s (equivalent to 1.5 *G*bps transmission rate) at the indoor measurement setup shown in Fig. 3.

As can be seen from Fig. 5, at high EIRP, the linearity of the active beamforming power amplifier is the limiting factor as the EVM increases at peak transmit powers. The EVM rise at the 60° azimuth steering angle takes place at lower EIRP compared to the broadside radiation because of antenna gain scan loss. This difference in EIRP is 4 dB, which is the measured gain difference between broadside and azimuth 60° steering angles (see Fig.2). It is worthwhile to note that when the phased array transmits at low EIRP, the SNR at the receiver limits the link performance. So we can see a good performance at both scanning angles. Hence, the EIRP dynamic range of the phased array is approximately 31 dB and 35 dB for 60° scan angle and broadside radiation, respectively, at EVM equal to 2 %. Clearly, if a higher EVM would be allowed, the EIRP dynamic range increases, but is limited by the maximum EIRP and the beamforming antenna gain scan loss.

Fig. 6 shows the EVM as a function of the scan angle for all possible combinations of measurements (except the ones employing attenuators) obtained by considering different QAM modulation orders, different IF (AWG) bandwidths of the modulated signals, and input signal voltage of the AWG as listed above. Each subplot represents the EVM as a function of the scan angle for the three IF (AWG) bandwidths and fixed modulation order and input signal voltage of the AWG. For example, Fig. 6(a) shows the results for the 16−QAM and input voltage of 200 mVpp. In Fig. 6, the modulation order increases from the left to the right columns, while the input voltage increases from the upper to the lower rows. Trends are maintained throughout all the measurements with a couple of exceptions due to corrupted data (see Fig. 6(i) and (m)). As expected, increasing the bandwidth of the modulated signals increases the EVM because more noise power is contained in the generated communications link signals as can be seen from each of the subplots Fig. 6. Also increasing the input signal voltage of the AWG, which is effectively increasing the EIRP, increases the EVM as can be seen, e.g., from Figs. 6(c), (g), (k) and (o) showing the EVM as a function of the scan angle

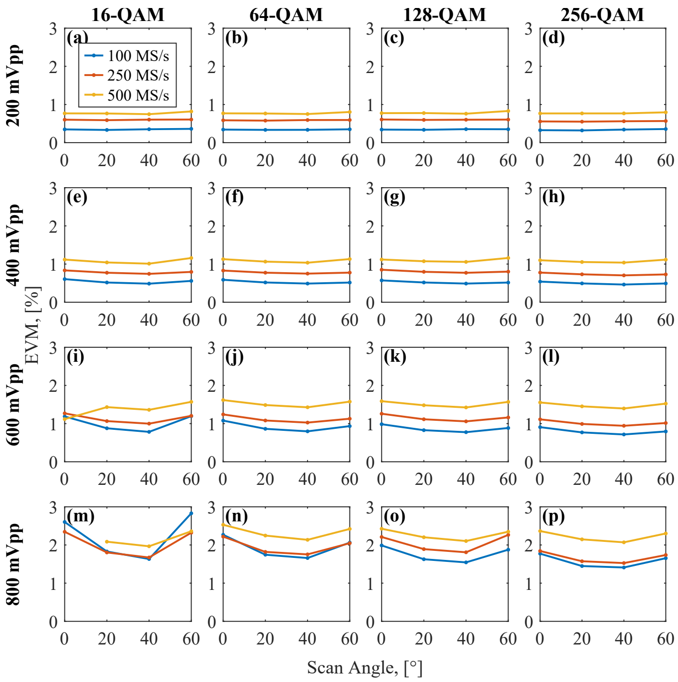

Fig. 6. TX EVM vs. scan angle measured over-the-air at a 3 m TX-RX separation for various modulated transmissions (increasing order from left to right) and various input signal voltages of the AWG (increasing order from the top down) at three transmission rates, i.e., 100, 250, 500 MS/s.

for the 128−QAM modulation. Another observation is that at lower (but still high) EIRP, or as presented here, at lower input signal voltage of the AWG, the EVM does not vary too much with the scan angle. On the other hand, the EIRP increases the EVM at broadside radiation and at the maximum scan angle are higher than at intermediate scan angles; compare Figs. 6(c) and (o). This is explained by the fact that stable performance is expected at the linear range of the power amplifiers while as the EIRP increases, it enters in the non-linear region. It is worthwhile to note that the corresponding EIRP values in all the plots in Fig. 6 vary between 45 and 60.5 dBm, which is rather high. Finally, a stable EVM performance is observed as the modulation order is increased for a fixed input voltage. Compare, e.g., Figs. 6(e), (f), (g), and (h) as the modulation order increases from 16−QAM to 256−QAM for a fixed input voltage of 200 mVpp.

V. Conclusion

Based on the presented measurements and analysis we have demonstrated the excellent transmit EVM performance of a slant-polarized 28 GHz gapwaveguide based phased array at 28 GHz. Results are based on non-standardized OTA link performance measurements for transmitting signals with various QAM modulation orders, symbol rates, and input powers. The results show that the phased array is capable of high data rate transmission at high EIRP. A 2.6% EVM was measured when transmitting modulated signals over a 3 Gbps link at 60.5 dB EIRP.

Acknowledgment

This work was partly supported by the European Union Horizon 2020 research and innovation program under the Marie Skłodowska-Curie grant agreement No. 766231 WAVE-COMBE H2020-MSCA-ITN-2017 and partly by Gapwaves AB.

References

[1] T. S. Rappaport et al., "Millimeter Wave Mobile Communications for 5G Cellular: It Will Work!," in IEEE Access, vol. 1, pp. 335-349, 2013, doi: 10.1109/ACCESS.2013.2260813.

[2] K. Kibaroglu, M. Sayginer, T. Phelps and G. M. Rebeiz, "A 64-Element 28-GHz Phased-Array Transceiver With 52-dBm EIRP and 8–12-Gb/s 5G Link at 300 Meters Without Any Calibration," in IEEE Transactions on Microwave Theory and Techniques, vol. 66, no. 12, pp. 5796-5811, Dec. 2018, doi: 10.1109/TMTT.2018.2854174.

[3] Y. Yin et al., "A 37–42-GHz 8 × 8 Phased-Array With 48–51-dBm EIRP, 64–QAM 30-Gb/s Data Rates, and EVM Analysis Versus Channel RMS Errors," in IEEE Transactions on Microwave Theory and Techniques, vol. 68, no. 11, pp. 4753-4764, Nov. 2020, doi: 10.1109/TMTT.2020.2998183.

[4] A. Bagheri, et al. (2022): A 16 × 16 45-degree Slant-Polarized Gapwaveguide Phased Array with 65 dBm EIRP at 28 GHz. TechRxiv. Preprint. https://doi.org/10.36227/techrxiv.21063058.v1

[5] E. Rajo-Iglesias, M. Ferrando-Rocher and A. U. Zaman, "Gap Waveguide Technology for Millimeter-Wave Antenna Systems," in IEEE Communications Magazine, vol. 56, no. 7, pp. 14-20, July 2018, doi: 10.1109/MCOM.2018.1700998.

[6] P.-S. Kildal, E. Alfonso, A. Valero-Nogueira and E. Rajo-Iglesias, "Local Metamaterial-Based Waveguides in Gaps Between Parallel Metal Plates," in IEEE Antennas and Wireless Propagation Letters, vol. 8, pp. 84-87, 2009, doi: 10.1109/LAWP.2008.2011147

[7] A. Bagheri, et al. (2022): A 28 GHz 8 × 8 Gapwaveguide Phased Array employing GaN Front-end with 60 dBm EIRP. TechRxiv. Preprint. https://doi.org/10.36227/techrxiv.21063103.v1

[8] 5G;NR;Base Station (BS) radio transmission and reception (3GPP TS 38.104 version 15.3.0 Release 15) ETSI TS 138 104 V15.3.0 (2018-10)http://www.etsi.org/standards-search

[9] AWMF-0153, 26.5-29.5 GHz Tx/Rx Up and Down Converter IFIC.Anokiwave.

[10] C. Bencivenni, T. Emanuelsson, and M. Gustafsson, "Gapwaves Platform Integrates 5G mmWave Arrays," Microwave Journal, vol. 62, no. 2, 2019.